ELSEVIER

Journal of Nuclear Materials 313–316 (2003) 873–877

journal of nuclear materials

www.elsevier.com/locate/jnucmat

Carbon sources in the DIII-D tokamak

R.C. Isler [a,*], R.J. Colchin [a], N.H. Brooks [b], T.E. Evans [b],
W.P. West [b], D.G. Whyte [c]

[a] *Oak Ridge National Laboratory (ORNL), Box 2009, Oak Ridge, TN 37831-8072, USA*
[b] *General Atomics, San Diego, CA 92186-5068, USA*
[c] *University of California at San Diego, San Diego, CA 92093, USA*

Abstract

Physical and chemical sputtering in the DIII-D divertors are distinguished by comparisons of emission rates of C I, CD, and C_2 radiation and by spectral profiles of C I lines. When flux measurements indicate chemical sputtering dominates, the effective C I temperatures (best fit to a thermal distribution) tend to lie in the range 1.0 ± 0.2 eV, as expected for atoms coming from molecular dissociation. When $P_{\text{inj}} \geqslant 7$ MW and $\bar{n}_e < 5 \times 10^{13}$ cm^{-3}, molecular emissions are very weak, if present at all, and effective C I temperatures reach values 5–7 eV. In these cases, detailed examinations of the C I line profiles often reveal that they are asymmetric with shifted peaks. Such characteristics are consistent with expectations for physical sputtering, and attempts have been made to understand the line shapes by modeling them using Thompson flux distributions.

PACS: 52.40.H
Keywords: Carbon production; Spectroscopy; Sputtering; Divertor; Carbon line profiles

---

1. Introduction

A great deal of research has been expended in studying plasma-graphite interactions that relate to carbon release in fusion devices. The most important of these mechanisms are physical sputtering, chemical sputtering, radiation-enhanced sublimation, and thermal sublimation. Conditions favoring the latter two processes are not usually realized in the DIII-D tokamak, so efforts to identify the active processes on the carbon tiles of the divertor targets have been aimed at distinguishing physical and chemical sputtering. The procedure relies on analyzing spectroscopic data to relate influxes of CD, and C_2 to the influx of C I and on correlating effective temperatures and detailed profiles of C I to those expected for the two different production mechanisms.

2. Experimental apparatus and viewing geometry

All the data analyzed for the present studies have been obtained from DIII-D tokamak operation employing either the upper single-null (USN) baffled divertor configuration shown in Fig. 1(a) or the lower single-null (LSN) open configuration illustrated in Fig. 1(b). Two quasi-vertical sets of spectrometer views onto the targets are available. Spectra in the 4000–9000 Å range are acquired by means of a 1.3 m Czerny–Turner spectrometer equipped with a 1200 l/mm grating. A two-dimensional CCD detector simultaneously records the input signals transmitted to the spectrometer through 12 optical fibers. The instrument function has a width corresponding to carbon atom temperatures of approximately 1 eV, and the entire system is calibrated so that absolute emission rates can be determined.

3. Fluxes and ion temperatures

The C I influx provides a measure of the total amount of carbon released from the divertor targets. It

---

[*] Corresponding author. Tel.: +1-865-574-1174; fax: +1-865-574-1191.
E-mail address: isler@fed.ornl.gov (R.C. Isler).

0022-3115/03/$ - see front matter © 2003 Elsevier Science B.V. All rights reserved.
PII: S0022-3115(02)01468-X

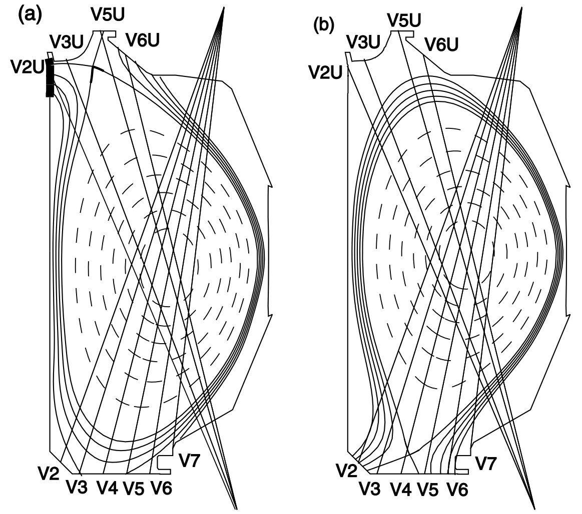

Fig. 1. Spectrometer views and typical magnetic configurations for (a) USN and (b) LSN operation.

can be produced directly by physical sputtering or by dissociation of molecules generated by chemical sputtering such as CD_4 or C_xD_y where x is 2 or 3 and y ranges from 2 to 6. Deciding whether or not chemical sputtering is the dominant process for a given type of operation depends on using the measured CD and C_2 fluxes to infer what fraction of the observed C I results from production of molecules. The procedure is described in detail in Ref. [1]. It relies on a mixture of theoretical [2,3] and experimental [4] results to obtain the expression

$$\Gamma^{\mathrm{mol}}_{\mathrm{C\,I}} = 52\Gamma_{C_2} + (\Gamma_{\mathrm{CD}} - 8\Gamma_{C_2}). \tag{1}$$

The first term on the right-hand side of Eq. (1) accounts for production of C_2D_y and C_3D_y and the second for production of CD_4 on the carbon tiles.

Total C I fluxes are obtained from the usual expression $\Gamma^{\mathrm{meas}}_{\mathrm{C\,I}} = IS/X$, where S and X are ionization and excitation rates calculated from a collisional-radiative model, and I is the intensity of a spectral multiplet. Uncertainties arise because the electron density and temperature at the location of the radiating atoms are not known. The temperature is assumed to be the same as the temperature of C II ions along the same view, and the density is usually taken as 10^{14} cm^{-3}, which is typical of locations near the divertor targets. The present analysis employs a readily observed ^3P–^3S multiplet, which has the most intense line at 9094.83 Å. Molecular fluxes are deduced from the CD 4300 Å system and the C_2 Swan system (5165 Å) by using a similar expression, suitably modified to account for populations of different vibrational levels. In practice, only two or three bands can usually be detected, but these seem to be sufficient to account for the influx in most applications since the molecular vibrational temperatures are low. Ordinarily, only a limited wavelength region of a molecular band can be measured, and it is necessary to model the rotational structure to infer the total intensity. In most cases, the rotational temperatures are of the order of 0.25 eV. CD and C_2 always appear together, but the dimer is easier to observe because the sensitivity of the detection system is greater at the longer wavelength.

Fluxes calculated from these emissions along view V2U (see Fig. 1) are shown in Fig. 2(a) together with an assessment of the C I flux from chemical sputtering calculated with Eq. (1). The neutral-beam power is 7.5 MW, and the line-averaged density reaches a peak value of 10^{14} cm^{-3}. It is clear that most of the carbon production arises from chemical sputtering, and in light of the uncertainties inherent in Eq. (1) and the differences in the three discharges used to record C I, CD, and C_2, it is possible to infer that all of the release may result from this process. In such cases, the effective C I temperatures

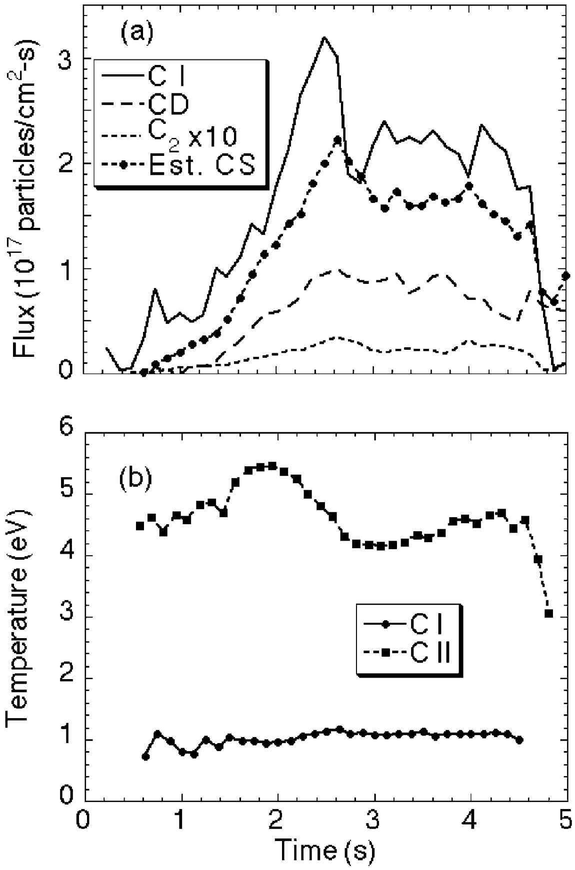

Fig. 2. (a) Atomic and molecular fluxes for a case where chemical sputtering appears to dominate. The estimated C I flux from chemical sputtering is close to the measured C I flux. (b) Typically observed ion temperatures in locations where chemical sputtering dominates.

obtained by fitting thermal distributions to the line shapes is 1.0 ± 0.2 eV, a value that is consistent with molecular dissociation as the source of atomic carbon. C II ion temperatures along the same view are 4–5 eV.

Discharges with neutral-beam power of 9 MW and a much lower line-averaged density of 3×10^{13} cm^{-3} produce quite different results along view V2U as shown in Fig. 3(a). Here, the molecular signatures are undetectable after about 2 s while the intensity of the C I signals and the inferred fluxes continue to increase up until the discharge is close to termination. Chemical sputtering seems to be operative only near the beginning of the discharge. Time histories of C I and C II temperatures reflect this change (Fig. 3(b)); they are low early in the shot but rise to much higher levels than is the case when chemical sputtering dominates. All indicators point to physical sputtering constituting the major release mechanism in this higher temperature plasma. Molecular emissions are always relatively weak when the C II temperature is above 10 eV.

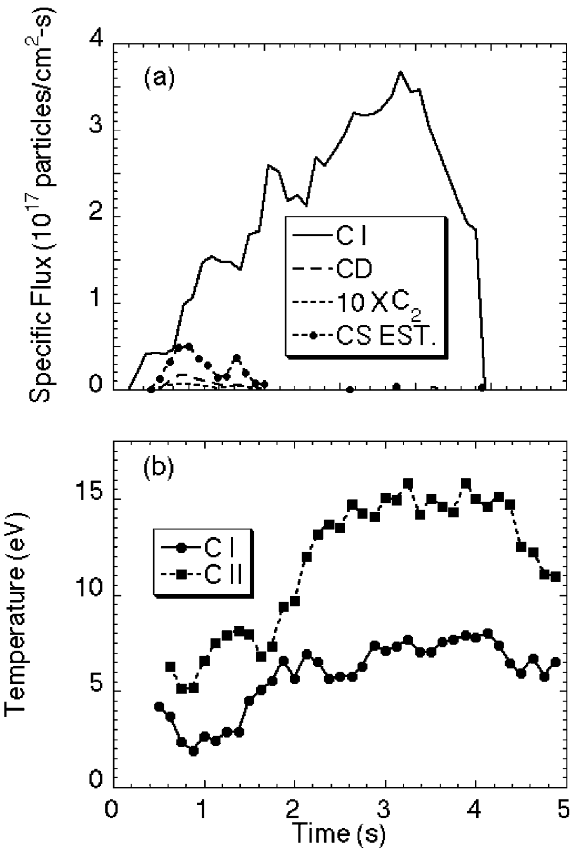

Fig. 3. (a) Atomic and molecular fluxes for a case where physical sputtering appears to dominate. Molecular emissions disappear early in the discharge. (b) Typically observed ion temperatures in locations where physical sputtering dominates.

4. C I line profiles

From the results shown in Figs. 2 and 3, it is tempting to adopt the high and low C I effective temperatures respectively as signatures of physical or chemical sputtering. Indeed, on close examination it is often observed that when the effective temperature is high, the lines are really asymmetric and the peaks are shifted; these characteristics are suggestive of sputtered particles. If the ionization time for sputtered carbon atoms from a divertor target is much shorter than their thermal relaxation time with the background plasma, excited C I lines should exhibit a strong blue wing, a weak red wing, and a shifted peak in the profile as a result of the particles moving principally toward the light collection optics. A red wing and shift of the peak intensity are predicted because the views are not strictly perpendicular to the carbon tiles. An additional shift may also appear if the distribution has an angular dependence such as $\cos\theta$, which is often associated with sputtering. In contrast, atoms produced by molecular breakup should exhibit only minor shifts and asymmetries.

In order to gain some additional insight into the physics of carbon release, the line shifts and shapes have been correlated to Thompson flux distributions [5] having a 'soft' cutoff (see Ref. [6], Eq. (14)) but no dependence on the ejection angle. The sputtering distribution in v and θ is converted to a distribution in $\Delta\lambda$ and θ from the Doppler shift relationship $\Delta\lambda = \lambda_0 \cos\theta v/c$, then integrated over the angles with appropriate limits for the viewing geometry to get a distribution in $\Delta\lambda$ alone.

$$f(\Delta\lambda)\,\mathrm{d}(\Delta\lambda) \propto \int \mathrm{d}\varphi \int \left[0.5m_{\mathrm{C}}\left(\frac{c\Delta\lambda}{\lambda_0\cos\theta}\right)^2 + U_0\right]^{-3} \times G(\Delta\lambda,\theta)\frac{\sin\theta}{\cos^4\theta}(\Delta\lambda)^3\,\mathrm{d}\theta\,\mathrm{d}(\Delta\lambda), \qquad (2)$$

$$G(\Delta\lambda,\theta) = 1 - \left[\left(0.5m_{\mathrm{C}}\left(\frac{c\Delta\lambda}{\lambda_0\cos\theta}\right)^2 + U_0\right) \Big/ \gamma(1-\gamma)E_{\mathrm{impact}}\right]^{1/2}, \qquad (3)$$

where

$$\gamma = \frac{4m_{\mathrm{D}}m_{\mathrm{C}}}{(m_{\mathrm{D}}+m_{\mathrm{C}})^2}.$$

Here, U_0 is the binding energy of carbon (7.4 eV), m_{D} and m_{C} are the masses of deuterium and carbon.

For comparison with experimental data it is first necessary to find the most probable profile of an emitted line. This is accomplished by deconvoluting the instrument function from the measurements using a maximum entropy routine. Results of such a deconvolution are

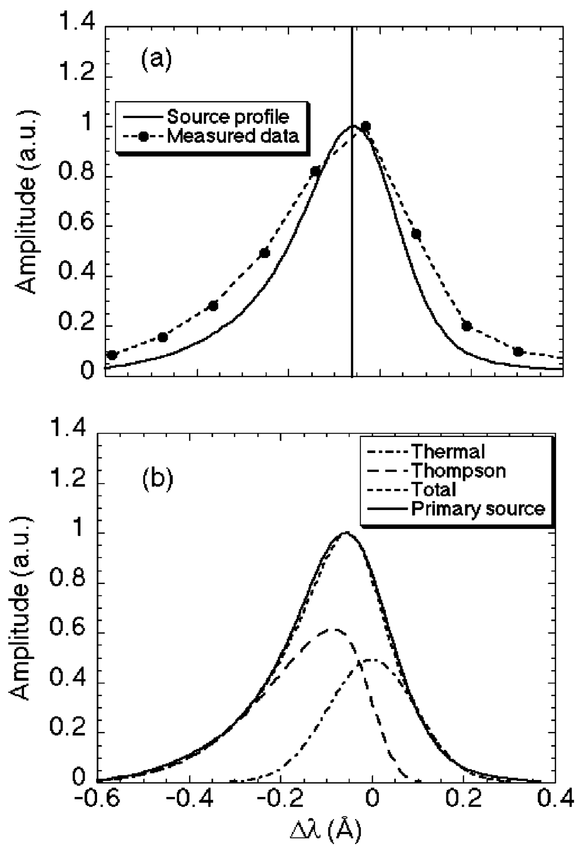

Fig. 4. (a) Measured profile (dashed line) and deconvoluted source profile (solid line) for a region exhibiting high effective C I temperatures. (b) Best fit to the source profile using a combination of Thompson (impact energy = 140 eV) and thermal (1.2 eV) distribution functions.

shown in Fig. 4(a). Data points are from view V5 (Fig. 1(b)) for the strongest component of the C I multiplet at 9094.83 Å. The asymmetry around the peak of the profile is obvious. The shift of the peak from the nominal line center has been measured by using the line profile at V2 as the fiducial; this profile appears undistorted around the peak, and strong molecular emissions in this view indicate most of the carbon is produced from molecular dissociation. The shift is −0.0533 Å, which corresponds to about one-half a pixel width of the CCD detector; the uncertainty is estimated to be ±0.01 Å. Accurate knowledge of the shifts are crucial for interpreting the data.

In Fig. 4(b) the spectroscopic data are compared to calculated profiles. While the red wing of the experimental measured line is attenuated, it is still too large to come solely from sputtered particles, and a thermal component has been added to reproduce this feature. A bombardment energy of 160 eV for the sputtered distribution and a temperature of 1.25 eV for the thermal component gives a good simulation of the measurement. Electron temperatures near the targets are in the neighborhood of 40 eV, so a 3 kT sheath would lead to impact energies approaching those implied from fitting the line profile. Whether the results of this modeling actually permit an accurate inference of the nature of the plasma-material interactions requires more extensive study, but the exploitation of C I line profiles to define the source mechanisms of carbon appears promising.

5. Summary

Although there are several uncertainties inherent in the derivation and application of Eq. (1), it appears to work well for discerning conditions where chemical sputtering is the dominant carbon release mechanism in the DIII-D divertors. This conclusion is reinforced by the observation that the effective C I temperatures are of the order of 1 eV when $\Gamma^{\text{meas}}_{\text{C I}} \approx \Gamma^{\text{molec}}_{\text{C I}}$. Similarly, in situations where molecular emissions are weak or not observed, the effective temperatures rise to the range of 5–7 eV, which seems to indicate physical sputtering activity. Thus, it appears possible to distinguish the release mechanism solely from effective temperature measurements, but detailed examination of the C I line shapes shows this conclusion may not be completely warranted. At high effective temperatures, the profiles are frequently asymmetric with shifted peaks when beam powers are in the 7–10 MW range. The profiles are best fit with a combination of a Thompson distribution, assuming impact energies reasonably consistent with 3 kT sheath potentials, and a very low temperature thermal distribution. The temperature of the thermal component agrees with observations from molecular dissociation and may indicate the presence of molecular sputtering even when the band emission is weak. However, the possibility that collisions between deuterons and carbon atoms are responsible for atleast part of the red wing cannot be ruled out. A broader set of studies is needed to put these inferences on a firmer basis.

Acknowledgements

This work has been supported by US DOE Fusion Contract DE-AC05-00OR22725, DE-AC03-99ER-54463, and Grant DE-FG03-95ER54294. We would like to thank Peter Stangeby for several helpful discussions concerning sputtering processes.

References

[1] R.C. Isler, R.J. Colchin, N.H. Brooks, T.E. Evans, W.P. West, D.G. Whyte, Phys. Plasmas 8 (2001) 4470.

[2] A. Pospieszczyk, Y. Ra, Y. Hirooka, R.W. Conn, D.M. Goebel, B. LaBombard, R.E. Nygren, Spectroscopic Studies of Carbon Containing Molecules and Their Breakup in PISCES-A, University of California at Los Angeles, Report UCLA-PPG-1251, 1989.

[3] A.B. Erhardt, W.D. Langer, Collisional Processes of Hydrocarbons in Hydrogen Plasmas, Princeton Plasma Physics Laboratory Report PPPL-2477, 1987.

[4] D.A. Alman, D.N. Ruzic, J.N. Brooks, Phys. Plasmas 7 (2000) 1421.

[5] M.W. Thompson, Philos. Mag. 18 (1968) 377.

[6] G. McCracken, P. Stott, Nucl. Fusion 19 (1979) 89.